IET Microwaves, Antennas & Propagation

Research Article

IET Journals
The Institution of Engineering and Technology

Alternative surface integral equation-based characteristic mode analysis of dielectric resonator antennas

ISSN 1751-8725
Received on 30th April 2015
Revised on 26th August 2015
Accepted on 13th September 2015
doi: 10.1049/iet-map.2015.0304
www.ietdl.org

Yikai Chen ✉

School of Electronic Engineering, University of Electronic Science and Technology of China, No. 2006, Xiyuan Ave, West Hi-Tech Zone, 611731 Chengdu, Sichuan, People's Republic of China
✉ *E-mail: ykchen@uestc.edu.cn*

Abstract: Dielectric resonator antennas are widely used in wireless communication systems. A theory of characteristic modes (CMs) for modal analysis of dielectric resonators is highly demanded. Although a few earlier studies had proposed CM theory for modelling scattering from dielectric bodies, the physical characteristics of these CMs and their eigenvalues are not as clear as that of those for conducting bodies. This study revisits the CM theory for dielectric resonators. Following the Poynting's theorem and the PMCHWT (Poggio, Miller, Chang, Harrington, Wu, and Tsai) equation, two generalised eigenvalue equations are formulated. The resultant eigenvalues possess clear physical meanings that are the same as those of perfectly electrically conducting problems. In addition, other possible CM formulations based on the PMCHWT equation are also discussed. Mathematical proofs are given in the Appendix to show how to formulate CM theory to physically describe the fundamental resonant modes of dielectric resonators. Numerical results are given to show the proposed CM formulations are effective in solving resonant frequencies and modal fields for dielectric resonators.

1 Introduction

Characteristic mode (CM) theory was initially proposed by Garbacz in 1965 [1] and was refined to an explicit formulation using the method of moments (MoM) [2]. It provides an elegant and useful approach to predict the resonant behaviour of perfectly electrically conducting (PEC) bodies [3–5]. Recently, it finds wide applications in a variety of antenna designs, including platform mounted antenna systems [6–10], multiple-input multiple-output handset antennas [11–13], circularly polarised microstrip antennas [14], reactively loaded antennas [15, 16], and ultra-wideband planar monopole antennas [17–19].

Early attempts to extend the CM theory to dielectric bodies were reported in [20, 21]. In [20], the CM theory was developed from the volume integral equation (VIE) for dielectric bodies. Harrington *et al.* commented on the VIE-based CM theory that the imaginary part of $\langle \boldsymbol{J}_n^*, \boldsymbol{Z}_{\mathrm{V}}\boldsymbol{J}_n \rangle$ was not the imaginary part of the complex power (Section II and IV of [20]), where $\boldsymbol{J}$ is the eigencurrent and $\boldsymbol{Z}_{\mathrm{V}}$ is the operator in the VIE. As $\langle \boldsymbol{J}_n^*, \boldsymbol{Z}_{\mathrm{V}}\boldsymbol{J}_n \rangle = 1 + \mathrm{j}\lambda_n$, where λ_n is the eigenvalue, it further illustrated that the eigenvalues solved from the VIE-based CM formulation did not represent the amount of energy stored in a scattering or radiation problem.

In [21], Chang and Harrington developed a CM formulation for dielectric bodies using surface integral equation (SIE). Scattering cross-sections of infinite circular and square cylinders were computed using the SIE-based CM formulation. However, the physical meanings of the eigenvalues in their SIE-based CM formulation were not interpreted. Therefore, Chang and Harrington concluded their work as follows [21]: 'Many questions are still left unanswered in the interpretation and application of characteristic modes to material objects. It is hoped that this work will be of some value to future researchers in their effort to gain a complete understanding of the theory of characteristic modes.' Hence, how to compute CMs of dielectric resonators with clear physical meanings becomes an open problem.

For arbitrarily shaped dielectric resonators, their modal analysis was conventionally conducted by seeking the roots of the determinant of the MoM impedance matrix in a complex frequency plane [22, 23]. However, as reported in [24], the numerical implementation of this method suffers from serious numerical issues and heavy computation burdens. First, a significant variation of the determinant appears only in a very narrow region around the resonant frequency. A very good initial guess of the root is required to ensure the convergence of the root searching procedure. However, a good initial guess of the root is generally unavailable. Second, root seeking must be conducted in a complex frequency plane. The root seeking along the imaginary frequency axis introduces heavy computational burden. Third, the modal currents are solved from a homogeneous matrix equation. As the right-hand side vector in the homogeneous matrix equation is a zero vector, neither of the Gaussian elimination nor more advanced solvers based on the singular value decomposition (SVD) work well for such homogeneous matrix equation. This problem becomes more serious when the number of unknowns increases. These issues prohibit the application of the determinant root seeking method in the dielectric resonator antenna designs. For these reasons, the determinant of the impedance matrix is abandoned in [24] since it is difficult to find its roots. Instead, Liu proposed to search the minimum of the reciprocal of the condition number of the impedance matrix in the complex frequency plane [24]. However, the modal field was still solved through SVD.

Recently, we have briefly reported an idea to solve CMs of dielectric bodies using SIE in a short conference paper [25]. To fully elaborate on how to develop CM formulations from the PMCHWT (Poggio, Miller, Chang, Harrington, Wu, and Tsai) formulations [26, 27], this paper addresses the key issues in the development of the CM formulation and the physical interpretations for the CMs of dielectric resonators. We focus on the following aspects in this study:

(i) Following the Poynting's theorem, we formulate two generalised eigenvalue equations by properly arranging the operators in the PMCHWT formulation. Physical meanings of the resultant eigenvalues are interpreted through rigorous mathematical derivations. As will be seen later, the eigenvalues in the newly developed CM formulations have the similar physical meanings as

those in the CM theory for PEC bodies. The eigenvalues indicate the amount of stored energy in a scattering or radiation problem. Numerical results are given to show the proposed CM formulations are effective and accurate in solving CMs of dielectric resonators.

(ii) There are another two possible generalised eigenvalue equations that can be derived from the PMCHWT formulation. Mathematical proofs and physical explanations are given in the Appendix to show why they cannot produce proper CMs with clear physical meanings.

In addition, as compared with the determinant root seeking method, the proposed CM formulations provide an efficient approach to compute resonant frequency of each radiating mode accurately. Specifically, the CM analysis avoids the frequency sweeping along the imaginary frequency axis. It also avoids solving homogeneous matrix equation. These features greatly enhance the computational efficiency of the CM analysis.

2 CM theory development

Let us consider a scattering problem with incident plane wave $(\boldsymbol{E}^{\text{inc}}, \boldsymbol{H}^{\text{inc}})$ illuminating a three-dimensional homogeneous dielectric body with volume V_2 and constitutive parameters (ε_2, μ_2). We assume the dielectric body is immersed in an unbounded homogeneous background medium with constitutive parameters (ε_1, μ_1). We denote the region of the homogeneous background as V_1. In addition, we denote the boundary surface of V_2 as S, and define $\hat{\boldsymbol{n}}$ as the unit normal vector pointing from region V_2 to V_1.

By invoking Love's equivalence principle [28], the scattering problem can be formulated in terms of an equivalent surface electric current $\boldsymbol{J} = \hat{\boldsymbol{n}} \times \boldsymbol{H}$ and an equivalent surface magnetic current $\boldsymbol{M} = \boldsymbol{E} \times \hat{\boldsymbol{n}}$ defined on the surface of the dielectric body S. Here, $\boldsymbol{E}$ and $\boldsymbol{H}$ are the total electric field and total magnetic field on S. The equivalent surface currents satisfy the PMCHWT formulations [26, 27]

$$\left[\eta_1 \mathcal{L}_1(\boldsymbol{J}) + \eta_2 \mathcal{L}_2(\boldsymbol{J}) - \mathcal{K}_1(\boldsymbol{M}) - \mathcal{K}_2(\boldsymbol{M})\right]_{\tan} = \boldsymbol{E}^{\text{inc}}_{\tan} \tag{1}$$

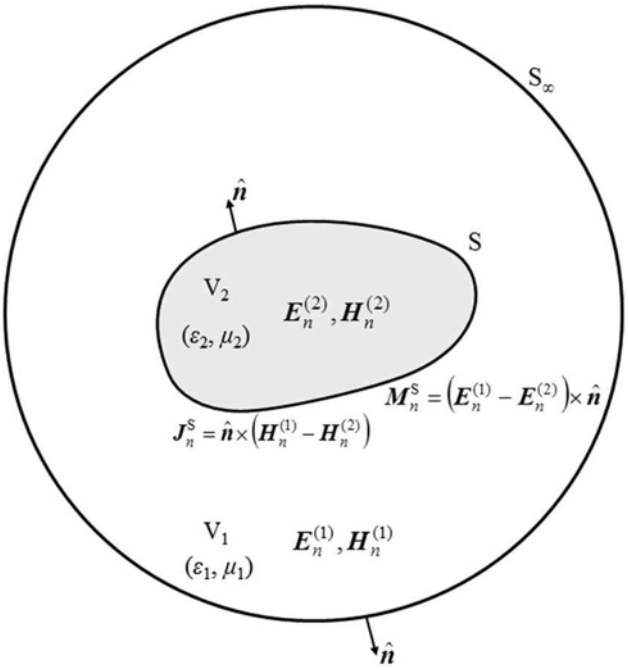

Fig. 1 *Configuration of the infinite radiation sphere and the outward unit normal vectors defined for regions V_1 and V_2*

$$\left[\mathcal{K}_1(\boldsymbol{J}) + \mathcal{K}_2(\boldsymbol{J}) + \frac{1}{\eta_1}\mathcal{L}_1(\boldsymbol{M}) + \frac{1}{\eta_2}\mathcal{L}_2(\boldsymbol{M})\right]_{\tan} = \boldsymbol{H}^{\text{inc}}_{\tan} \tag{2}$$

where $\eta_i = \sqrt{\mu_i/\varepsilon_i}$ is the intrinsic impedance in region V_i. The operators $\mathcal{L}_i$ and $\mathcal{K}_i$ are defined as

$$\mathcal{L}_i(\boldsymbol{X}) = \mathrm{j}k_i \int_S \left(\mathcal{I} + \frac{\nabla\nabla}{k_i^2}\right) G(\boldsymbol{r}, \boldsymbol{r}'; k_i) \cdot \boldsymbol{X}(\boldsymbol{r}')\, \mathrm{d}\boldsymbol{r}' \tag{3}$$

$$\mathcal{K}_i(\boldsymbol{X}) = \text{P.V.} \int_S \boldsymbol{X}(\boldsymbol{r}') \times \nabla G(\boldsymbol{r}, \boldsymbol{r}'; k_i)\, \mathrm{d}\boldsymbol{r}' \tag{4}$$

where k_i is the wavenumber in region V_i, $G(\boldsymbol{r}, \boldsymbol{r}'; k_i)$ is the Green's function in an unbounded homogeneous medium with the wavenumber k_i, and $\mathcal{I}$ is the identity operator. In (4), P.V. denotes the Cauchy principal value of the integration. Define the following new operators

$$\mathcal{Z}^{E\mathcal{J}} = \left(\eta_1 \mathcal{L}_1 + \eta_2 \mathcal{L}_2\right)_{\tan} \tag{5}$$

$$\mathcal{Z}^{E\mathcal{M}} = \left(-\mathcal{K}_1 - \mathcal{K}_2\right)_{\tan} \tag{6}$$

$$\mathcal{Z}^{\mathcal{H}\mathcal{J}} = \left(\mathcal{K}_1 + \mathcal{K}_2\right)_{\tan} \tag{7}$$

$$\mathcal{Z}^{\mathcal{H}\mathcal{M}} = \left(\tfrac{1}{\eta_1}\mathcal{L}_1 + \tfrac{1}{\eta_2}\mathcal{L}_2\right)_{\tan} \tag{8}$$

The PMCHWT formulations can be written in a more compact form

$$\mathcal{Z}^{E\mathcal{J}}\boldsymbol{J} + \mathcal{Z}^{E\mathcal{M}}\boldsymbol{M} = \boldsymbol{E}^{\text{inc}}_{\tan} \tag{9}$$

$$\mathcal{Z}^{\mathcal{H}\mathcal{J}}\boldsymbol{J} + \mathcal{Z}^{\mathcal{H}\mathcal{M}}\boldsymbol{M} = \boldsymbol{H}^{\text{inc}}_{\tan} \tag{10}$$

The following four points have to be kept in mind throughout the developments in this study:

(i) Only one impressed field $(\boldsymbol{E}^{\text{inc}}, \boldsymbol{H}^{\text{inc}})$ is presented in the scattering problem. This impressed field is the actual source that supplies power to the scattering problem. There is no other actual source that contributes power to the scattering problem.

(ii) The equivalent surface electric current $\boldsymbol{J}$ and equivalent surface magnetic current $\boldsymbol{M}$ are the equivalent surface currents to give the exactly same fields in regions V_1 and V_2. These two equivalent surface currents do not supply power to the scattering problem.

(iii) In the CM theory of dielectric bodies, we intend to solve the characteristic equivalent surface currents on the equivalent surface S, which can clearly describe the fundamental (resonant) modes of the dielectric resonators at their resonant frequencies. These characteristic currents are a complete and orthogonal current set that can be used to expand any equivalent surface currents caused by arbitrary actual impressed sources.

(iv) The characteristic currents and characteristic fields in CM theory exist in a source-free problem. No actual impressed source is considered in the solving of CMs for dielectric bodies.

Define $\boldsymbol{J}_n$ and $\boldsymbol{M}_n$ as the characteristic equivalent surface currents on the surface S of a dielectric body, where the subscript n denotes they are the characteristic equivalent surface currents of the nth order CM. They produce characteristic magnetic fields $\boldsymbol{H}_n^{(i)}$ and characteristic electric fields $\boldsymbol{E}_n^{(i)}$ in region V_i $(i = 1, 2)$. As CMs exist without any actual impressed sources [1, 2, 21], the characteristic currents satisfy the following equations on S as shown in Fig. 1

$$\mathcal{Z}^{E\mathcal{J}}\boldsymbol{J}_n + \mathcal{Z}^{E\mathcal{M}}\boldsymbol{M}_n = -\left(\boldsymbol{E}_n^{(1)} - \boldsymbol{E}_n^{(2)}\right)_{\tan} \tag{11}$$

$$\mathcal{Z}^{\mathcal{H}\mathcal{J}}\boldsymbol{J}_n + \mathcal{Z}^{\mathcal{H}\mathcal{M}}\boldsymbol{M}_n = -\left(\boldsymbol{H}_n^{(1)} - \boldsymbol{H}_n^{(2)}\right)_{\tan} \tag{12}$$

It should be noted that the characteristic equivalent surface currents $\boldsymbol{J}_n$ and $\boldsymbol{M}_n$ only satisfy the generalised eigenvalue

IET Microw. Antennas Propag., 2016, Vol. 10, Iss. 2, pp. 193–201

equation resulted from (9) and (10) under source-free condition. Under the source-free condition, the CM analysis for PEC structures [2] and dielectric structures as discussed in this paper does not consider any excitation at all. This is quite different from the zero excitation condition in [22–24], where the modal fields were solved from a homogeneous equation with a zero right-hand side vector. Owing to the source-free condition, the characteristic fields may not necessarily satisfy the boundary conditions. This difference makes the CMs differ with the natural modes (resulted from zero excitation condition) as defined in [22–24].

To ensure the characteristic currents have clear physical meanings and keep the intrinsic relationships between the equivalent currents, (11) and (12) need proper constrains. As shown in Fig. 1, two sets of surface currents are defined from the differences of the fields across the equivalent surface S

$$\boldsymbol{J}_n^S = \hat{\boldsymbol{n}} \times \left(\boldsymbol{H}_n^{(1)} - \boldsymbol{H}_n^{(2)}\right) \tag{13}$$

$$\boldsymbol{M}_n^S = \left(\boldsymbol{E}_n^{(1)} - \boldsymbol{E}_n^{(2)}\right) \times \hat{\boldsymbol{n}} \tag{14}$$

Let $\boldsymbol{J}_n^S = 0$ on surface S, it ensures the magnetic fields are continuous across the interface between regions V_1 and V_2. From (12), we have

$$\boldsymbol{M}_n = -(\mathcal{Z}^{\mathcal{HM}})^{-1}\mathcal{Z}^{\mathcal{HJ}}\boldsymbol{J}_n \tag{15}$$

Substituting (15) into (11), we have

$$\mathcal{Z}^{E\mathcal{J}}\boldsymbol{J}_n + \mathcal{Z}^{E\mathcal{M}}\boldsymbol{M}_n = \left(\mathcal{Z}^{E\mathcal{J}} - \mathcal{Z}^{E\mathcal{M}}(\mathcal{Z}^{\mathcal{HM}})^{-1}\mathcal{Z}^{\mathcal{HJ}}\right)\boldsymbol{J}_n = \mathcal{Z}^E\boldsymbol{J}_n \tag{16}$$

where $\mathcal{Z}^E = \mathcal{Z}^{E\mathcal{J}} - \mathcal{Z}^{E\mathcal{M}}(\mathcal{Z}^{\mathcal{HM}})^{-1}\mathcal{Z}^{\mathcal{HJ}}$. Owing to the symmetry of the operators $\mathcal{Z}^{E\mathcal{J}}$, $\mathcal{Z}^{E\mathcal{M}}$, $\mathcal{Z}^{\mathcal{HJ}}$, and $\mathcal{Z}^{\mathcal{HM}}$, and also because of $\mathcal{Z}^{E\mathcal{M}} = -\mathcal{Z}^{\mathcal{HJ}}$, one can get

$$(\mathcal{Z}^E)^{\mathrm{T}} = \mathcal{Z}^E \tag{17}$$

where the superscript 'T' denotes the transpose of the operator in the bracket. Therefore, $\mathcal{Z}^E$ is a symmetric operator. It can be expressed in terms of Hermitian parts as $\mathcal{Z}^E = \mathcal{R}^E + \mathrm{j}\mathcal{X}^E$, where

$$\mathcal{R}^E = \tfrac{1}{2}\left(\mathcal{Z}^E + (\mathcal{Z}^E)^*\right) \tag{18}$$

$$\mathcal{X}^E = \tfrac{1}{2j}\left(\mathcal{Z}^E - (\mathcal{Z}^E)^*\right) \tag{19}$$

where the asterisk denotes the complex conjugate.

As there is no actual impressed source inside region V_1, the net complex power is zero. Following the Poynting's theorem in source-free region [29], we have

$$P^{(1)} = \int_{S+S_\infty} \boldsymbol{E}_n^{(1)} \times (\boldsymbol{H}_n^{(1)})^* \mathrm{d}\boldsymbol{S} + \mathrm{j}\omega \int_{V_1} \left(\mu_1 |\boldsymbol{H}_n^{(1)}|^2 - \varepsilon_1 |\boldsymbol{E}_n^{(1)}|^2\right) \mathrm{d}V = 0 \tag{20}$$

where S_∞ denotes the infinite radiation sphere as shown in Fig. 1. The first term on the right side gives the complex power entering the region V_1 from its environment; the second term on the right side represents the complex power stored in the region V_1. Taking the definition of the outward normal unit vector for surfaces S and S_∞, (20) can be further written as

$$P^{(1)} = -\int_S \boldsymbol{E}_n^{(1)} \times (\boldsymbol{H}_n^{(1)})^* \cdot \hat{\boldsymbol{n}}\, \mathrm{d}S + \int_{S_\infty} \boldsymbol{E}_n^{(1)} \times (\boldsymbol{H}_n^{(1)})^* \cdot \hat{\boldsymbol{n}}\, \mathrm{d}S + \mathrm{j}\omega \int_{V_1} \left(\mu_1 |\boldsymbol{H}_n^{(1)}|^2 - \varepsilon_1 |\boldsymbol{E}_n^{(1)}|^2\right) \mathrm{d}V = 0 \tag{21}$$

Therefore

$$\int_S \boldsymbol{E}_n^{(1)} \times (\boldsymbol{H}_n^{(1)})^* \cdot \hat{\boldsymbol{n}}\, \mathrm{d}S = \int_{S_\infty} \boldsymbol{E}_n^{(1)} \times (\boldsymbol{H}_n^{(1)})^* \cdot \hat{\boldsymbol{n}}\, \mathrm{d}S + \mathrm{j}\omega \int_{V_1} \left(\mu_1 |\boldsymbol{H}_n^{(1)}|^2 - \varepsilon_1 |\boldsymbol{E}_n^{(1)}|^2\right) \mathrm{d}V \tag{22}$$

Similarly, there is also no actual impressed source inside region V_2. Following the Poynting's theorem in source-free region V_2 [29], we have

$$P^{(2)} = \int_S \boldsymbol{E}_n^{(2)} \times (\boldsymbol{H}_n^{(2)})^* \cdot \hat{\boldsymbol{n}}\, \mathrm{d}S + \mathrm{j}\omega \int_{V_2} \left(\mu_2 |\boldsymbol{H}_n^{(2)}|^2 - \varepsilon_2 |\boldsymbol{E}_n^{(2)}|^2\right) \mathrm{d}V = 0 \tag{23}$$

Therefore, we have

$$-\int_S \boldsymbol{E}_n^{(2)} \times (\boldsymbol{H}_n^{(2)})^* \cdot \hat{\boldsymbol{n}}\, \mathrm{d}S = \mathrm{j}\omega \int_{V_2} \left(\mu_2 |\boldsymbol{H}_n^{(2)}|^2 - \varepsilon_2 |\boldsymbol{E}_n^{(2)}|^2\right) \mathrm{d}V \tag{24}$$

Adding (22)–(24) yields

$$\int_S \boldsymbol{E}_n^{(1)} \times (\boldsymbol{H}_n^{(1)})^* \cdot \hat{\boldsymbol{n}}\, \mathrm{d}S - \int_S \boldsymbol{E}_n^{(2)} \times (\boldsymbol{H}_n^{(2)})^* \cdot \hat{\boldsymbol{n}}\, \mathrm{d}S = \int_{S_\infty} \boldsymbol{E}_n^{(1)} \times (\boldsymbol{H}_n^{(1)})^* \cdot \hat{\boldsymbol{n}}\, \mathrm{d}S + \mathrm{j}\omega \int_{V_1} \left(\mu_1 |\boldsymbol{H}_n^{(1)}|^2 - \varepsilon_1 |\boldsymbol{E}_n^{(1)}|^2\right) \mathrm{d}V + \mathrm{j}\omega \int_{V_2} \left(\mu_2 |\boldsymbol{H}_n^{(2)}|^2 - \varepsilon_2 |\boldsymbol{E}_n^{(2)}|^2\right) \mathrm{d}V \tag{25}$$

Using (16), $\boldsymbol{J}_n^S = 0$ and the vector identity $(\boldsymbol{a} \times \boldsymbol{b}) \cdot \boldsymbol{c} = (\boldsymbol{b} \times \boldsymbol{c}) \cdot \boldsymbol{a} = (\boldsymbol{c} \times \boldsymbol{a}) \cdot \boldsymbol{b}$, we have

$$\begin{aligned}
&\int_S \boldsymbol{E}_n^{(1)} \times (\boldsymbol{H}_n^{(1)})^* \cdot \hat{\boldsymbol{n}}\, \mathrm{d}S - \int_S \boldsymbol{E}_n^{(2)} \times (\boldsymbol{H}_n^{(2)})^* \cdot \hat{\boldsymbol{n}}\, \mathrm{d}S \\
&= \int_S \boldsymbol{E}_n^{(1)} \cdot ((\boldsymbol{H}_n^{(1)})^* \times \hat{\boldsymbol{n}})\, \mathrm{d}S - \int_S \boldsymbol{E}_n^{(2)} \cdot ((\boldsymbol{H}_n^{(2)})^* \times \hat{\boldsymbol{n}})\, \mathrm{d}S \\
&= \int_S (\boldsymbol{E}_n^{(1)} - \boldsymbol{E}_n^{(2)}) \cdot ((\boldsymbol{H}_n^{(1)})^* \times \hat{\boldsymbol{n}})\, \mathrm{d}S \\
&= -\int_S (\boldsymbol{E}_n^{(1)} - \boldsymbol{E}_n^{(2)})_{\tan} \cdot (\boldsymbol{J}_n)^*\, \mathrm{d}S \\
&= \langle (\boldsymbol{J}_n)^*, \mathcal{Z}^E \boldsymbol{J}_n \rangle
\end{aligned} \tag{26}$$

where the inner product is defined for the Hilbert space on the equivalent surface S. Applying (25) and $\mathcal{Z}^E = \mathcal{R}^E + \mathrm{j}\mathcal{X}^E$ to (26), we have

$$\begin{aligned}
P^{\text{total}} &= \langle (\boldsymbol{J}_n)^*, \mathcal{Z}^E \boldsymbol{J}_n \rangle = \langle \boldsymbol{J}_n^*, (\mathcal{R}^E + \mathrm{j}\mathcal{X}^E)\boldsymbol{J}_n \rangle \\
&= \langle \boldsymbol{J}_n^*, \mathcal{R}^E \boldsymbol{J}_n \rangle + \mathrm{j}\langle \boldsymbol{J}_n^*, \mathcal{X}^E \boldsymbol{J}_n \rangle \\
&= \int_{S_\infty} \boldsymbol{E}_n^{(1)} \times (\boldsymbol{H}_n^{(1)})^* \cdot \hat{\boldsymbol{n}}\, \mathrm{d}S + \mathrm{j}\omega \int_{V_1} \left(\mu_1 |\boldsymbol{H}_n^{(1)}|^2 - \varepsilon_1 |\boldsymbol{E}_n^{(1)}|^2\right) \mathrm{d}V \\
&\quad + \mathrm{j}\omega \int_{V_2} \left(\mu_2 |\boldsymbol{H}_n^{(2)}|^2 - \varepsilon_2 |\boldsymbol{E}_n^{(2)}|^2\right) \mathrm{d}V
\end{aligned} \tag{27}$$

where $\int_{S_\infty} \boldsymbol{E}_n^{(1)} \times (\boldsymbol{H}_n^{(1)})^* \cdot \hat{\boldsymbol{n}}\, \mathrm{d}S$ represents the radiation power on the

infinite radiation sphere S_∞. The last two terms in (27) are imaginary power. They represent the energies stored in regions V_1 and V_2, respectively. Evidently, $\langle \boldsymbol{J}_n^*, \mathcal{R}^E \boldsymbol{J}_n \rangle$ and $\langle \boldsymbol{J}_n^*, \mathcal{X}^E \boldsymbol{J}_n \rangle$ give the radiation and stored energy, respectively. $\langle \boldsymbol{J}_n^*, \mathcal{R}^E \boldsymbol{J}_n \rangle$ cannot be negative as radiated power must be greater than zero or equal to zero. Therefore, $\mathcal{R}^E$ is a semi-positive definite operator.

To achieve high radiation efficiency in a radiation system, we intend to improve the radiation power and reduce the stored energy within the radiation system. Mathematically, we can achieve high radiation efficiency by minimising the following function:

$$f(\boldsymbol{J}_n) = \frac{P_{\text{store}}}{P_{\text{radiation}}} = \frac{\langle \boldsymbol{J}_n^*, \mathcal{X}^E \boldsymbol{J}_n \rangle}{\langle \boldsymbol{J}_n^*, \mathcal{R}^E \boldsymbol{J}_n \rangle} \tag{28}$$

A variational expression in terms of $\boldsymbol{J}_n$ immediately gives the following generalised eigenvalue equation

$$\mathcal{X}^E \boldsymbol{J}_n = \lambda_n \mathcal{R}^E \boldsymbol{J}_n \tag{29}$$

As both $\mathcal{R}^E$ and $\mathcal{X}^E$ are symmetric operators, all the eigenvalues λ_n and characteristic currents $\boldsymbol{J}_n$ must be real. Therefore

$$\begin{aligned} \langle \boldsymbol{J}_n^*, (\mathcal{R}^E + \mathrm{j}\mathcal{X}^E)\boldsymbol{J}_n \rangle &= \langle \boldsymbol{J}_n, (\mathcal{R}^E + \mathrm{j}\mathcal{X}^E)\boldsymbol{J}_n \rangle \\ &= (1 + \mathrm{j}\lambda_n)\langle \boldsymbol{J}_n, \mathcal{R}^E \boldsymbol{J}_n \rangle \end{aligned} \tag{30}$$

In general, the eigenvalues range from $-\infty$ to $+\infty$. As $\langle \boldsymbol{J}_n^*, \mathcal{R}^E \boldsymbol{J}_n \rangle$ represents the radiation power of the system, (30) shows that the magnitude of eigenvalue $|\lambda_n|$ is the ratio between the stored energy and the radiation power. By comparing (27) and (30), we also find that CMs with $\lambda_n > 0$ are inductive modes, and those with $\lambda_n < 0$ are capacitive modes. Particularly, CMs with $\lambda_n = 0$ are externally resonant modes, which is indicating that there is no net energy stored in a radiation or scattering problem. As compared with the CM theory for PEC bodies [2], physical meanings of the eigenvalues solved from (29) are the same as that for PEC problems.

Each characteristic current $\boldsymbol{J}_n$ can be normalised such that it radiates unit power

$$\langle \boldsymbol{J}_n, \mathcal{R}^E \boldsymbol{J}_n \rangle = 1 \tag{31}$$

After normalisation, the orthogonality relationship among characteristic currents $\boldsymbol{J}_n$ is given by

$$\langle \boldsymbol{J}_m, \mathcal{Z}^E \boldsymbol{J}_n \rangle = (1 + \mathrm{j}\lambda_n)\delta_{mn} \tag{32}$$

where δ_{mn} is the Kronecker delta function (0 if $m \neq n$, and 1 if $m = n$).

Consider the normalised characteristic currents $\boldsymbol{J}_n$, from (27) and (30), we can obtain

$$\begin{aligned} &\int_{S_\infty} \boldsymbol{E}_m^{(1)} \times (\boldsymbol{H}_n^{(1)})^* \cdot \hat{\boldsymbol{n}}\, \mathrm{dS} + \mathrm{j}\omega \int_{V_1} \left(\mu_1 |\boldsymbol{H}_m^{(1)}|^2 - \varepsilon_1 |\boldsymbol{E}_n^{(1)}|^2 \right) \mathrm{d}\tau \\ &\quad + \mathrm{j}\omega \int_{V_2} \left(\mu_2 |\boldsymbol{H}_m^{(2)}|^2 - \varepsilon_2 |\boldsymbol{E}_n^{(2)}|^2 \right) \mathrm{d}\tau \\ &\quad = (1 + \mathrm{j}\lambda_n)\delta_{mn} \end{aligned} \tag{33}$$

where the quantities with subscript 'm' denotes they are associated with the mth CM. As the characteristic fields are outward travelling waves on the infinite radiation sphere S_∞, they satisfy

$$\boldsymbol{E}_n^{(1)} = \eta_1 \boldsymbol{H}_n^{(1)} \times \hat{\boldsymbol{n}} \tag{34}$$

Substituting (34) into (33) and adding (33) to its conjugate with m and n interchanged, we have

$$\frac{1}{\eta_1} \int_{S_\infty} \boldsymbol{E}_m^{(1)} \cdot (\boldsymbol{E}_n^{(1)})^* \cdot \hat{\boldsymbol{n}}\, \mathrm{dS} = \delta_{mn} \tag{35}$$

It shows that the resultant characteristic fields are orthogonal with each other on S_∞.

3 Alternative CM formulation

The generalised eigenvalue equation in (29) is defined in terms of the equivalent surface electric current. The development of a dual form of (29) is addressed in this section. Let $\boldsymbol{M}_n^S = 0$ on surface S, it ensures the electric fields are continuous across the interface of regions V_1 and V_2. From (11), we have

$$\boldsymbol{J}_n = -(\mathcal{Z}^{E\mathcal{J}})^{-1} \mathcal{Z}^{E\mathcal{M}} \boldsymbol{M}_n \tag{36}$$

Substituting (36) into (12), we have

$$\begin{aligned} \mathcal{Z}^{\mathcal{H}\mathcal{J}} \boldsymbol{J}_n + \mathcal{Z}^{\mathcal{H}\mathcal{M}} \boldsymbol{M}_n &= \left(\mathcal{Z}^{\mathcal{H}\mathcal{M}} - \mathcal{Z}^{\mathcal{H}\mathcal{J}} (\mathcal{Z}^{E\mathcal{J}})^{-1} \mathcal{Z}^{E\mathcal{M}} \right) \boldsymbol{M}_n \\ &= \mathcal{Z}^{\mathcal{M}} \boldsymbol{M}_n \end{aligned} \tag{37}$$

where $\mathcal{Z}^{\mathcal{M}} = \mathcal{Z}^{\mathcal{H}\mathcal{M}} - \mathcal{Z}^{\mathcal{H}\mathcal{J}} (\mathcal{Z}^{E\mathcal{J}})^{-1} \mathcal{Z}^{E\mathcal{M}}$

As $\mathcal{Z}^{E\mathcal{J}}$, $\mathcal{Z}^{E\mathcal{M}}$, $\mathcal{Z}^{\mathcal{H}\mathcal{J}}$, and $\mathcal{Z}^{\mathcal{H}\mathcal{M}}$ are symmetric, and $\mathcal{Z}^{E\mathcal{M}} = -\mathcal{Z}^{\mathcal{H}\mathcal{J}}$, it is easy to find that $\mathcal{Z}^{\mathcal{M}}$ is a symmetric operator. It can be expressed in terms of Hermitian parts as $\mathcal{Z}^{\mathcal{M}} = \mathcal{R}^{\mathcal{M}} + \mathrm{j}\mathcal{X}^{\mathcal{M}}$, where

$$\mathcal{R}^{\mathcal{M}} = \tfrac{1}{2} \left(\mathcal{Z}^{\mathcal{M}} + (\mathcal{Z}^{\mathcal{M}})^* \right) \tag{38}$$

$$\mathcal{X}^{\mathcal{M}} = \tfrac{1}{2j} \left(\mathcal{Z}^{\mathcal{M}} - (\mathcal{Z}^{\mathcal{M}})^* \right) \tag{39}$$

Using the (37), $\boldsymbol{M}_n^S = 0$ and the vector identity $(\boldsymbol{a} \times \boldsymbol{b}) \cdot \boldsymbol{c} = (\boldsymbol{b} \times \boldsymbol{c}) \cdot \boldsymbol{a} = (\boldsymbol{c} \times \boldsymbol{a}) \cdot \boldsymbol{b}$, we obtain

$$\begin{aligned} &\int_S \boldsymbol{E}_n^{(1)} \times (\boldsymbol{H}_n^{(1)})^* \cdot \hat{\boldsymbol{n}}\, \mathrm{d}S - \int_S \boldsymbol{E}_n^{(2)} \times (\boldsymbol{H}_n^{(2)})^* \cdot \hat{\boldsymbol{n}}\, \mathrm{d}S \\ &\quad = \int_S (\hat{\boldsymbol{n}} \times \boldsymbol{E}_n^{(1)}) \cdot (\boldsymbol{H}_n^{(1)})^* \, \mathrm{d}S - \int_S (\hat{\boldsymbol{n}} \times \boldsymbol{E}_n^{(2)}) \cdot (\boldsymbol{H}_n^{(2)})^* \, \mathrm{d}S \\ &\quad = -\int_S (\boldsymbol{H}_n^{(1)} - \boldsymbol{H}_n^{(2)})^* \cdot ((\boldsymbol{E}_n^{(1)}) \times \hat{\boldsymbol{n}}) \, \mathrm{d}S \\ &\quad = -\int_S (\boldsymbol{H}_n^{(1)} - \boldsymbol{H}_n^{(2)})_{\tan}^* \cdot \boldsymbol{M}_n \, \mathrm{d}S \\ &\quad = \langle (\mathcal{Z}^{\mathcal{M}} \boldsymbol{M}_n)*, \boldsymbol{M}_n \rangle \end{aligned} \tag{40}$$

Following (25) and (40), we have

$$\begin{aligned} \langle (\mathcal{Z}^{\mathcal{M}} \boldsymbol{M}_n)*, \boldsymbol{M}_n \rangle = &\int_{S_\infty} \boldsymbol{E}_n^{(1)} \times (\boldsymbol{H}_n^{(1)})^* \cdot \hat{\boldsymbol{n}}\, \mathrm{d}S \\ &+ \mathrm{j}\omega \int_{V_1} \left(\mu_1 |\boldsymbol{H}_n^{(1)}|^2 - \varepsilon_1 |\boldsymbol{E}_n^{(1)}|^2 \right) \mathrm{d}V \\ &+ \mathrm{j}\omega \int_{V_2} \left(\mu_2 |\boldsymbol{H}_n^{(2)}|^2 - \varepsilon_2 |\boldsymbol{E}_n^{(2)}|^2 \right) \mathrm{d}V \end{aligned} \tag{41}$$

IET Microw. Antennas Propag., 2016, Vol. 10, Iss. 2, pp. 193–201

Applying $\mathcal{Z}^{\mathcal{M}} = \mathcal{R}^{\mathcal{M}} + \mathrm{j}\mathcal{X}^{\mathcal{M}}$ to (41), we have

$$\begin{aligned} P^{\text{total}} &= \langle \boldsymbol{M}_n^*, \mathcal{Z}^{\mathcal{M}} \boldsymbol{M}_n \rangle \\ &= \langle \boldsymbol{M}_n^*, (\mathcal{R}^{\mathcal{M}} + \mathrm{j}\mathcal{X}^{\mathcal{M}}) \boldsymbol{M}_n \rangle \\ &= \langle \boldsymbol{M}_n^*, \mathcal{R}^{\mathcal{M}} \boldsymbol{M}_n \rangle + \mathrm{j} \langle \boldsymbol{M}_n^*, \mathcal{X}^{\mathcal{M}} \boldsymbol{M}_n \rangle \\ &= \langle (\mathcal{Z}^{\mathcal{M}} \boldsymbol{M}_n)^*, \boldsymbol{M}_n \rangle^* \\ &= \left[\int_{S_\infty} \boldsymbol{E}_n^{(1)} \times (\boldsymbol{H}_n^{(1)})^* \cdot \hat{\boldsymbol{n}} \, \mathrm{d}S + \mathrm{j}\omega \int_{V_1} \left(\mu_1 |\boldsymbol{H}_n^{(1)}|^2 - \varepsilon_1 |\boldsymbol{E}_n^{(1)}|^2 \right) \mathrm{d}V \right. \\ &\quad \left. + \mathrm{j}\omega \int_{V_2} \left(\mu_2 |\boldsymbol{H}_n^{(2)}|^2 - \varepsilon_2 |\boldsymbol{E}_n^{(2)}|^2 \right) \mathrm{d}V \right]^* \end{aligned} \tag{42}$$

Similar to the discussions in Section 2, the surface integral $\int_{S_\infty} (\boldsymbol{E}_n^{(1)})^* \times (\boldsymbol{H}_n^{(1)}) \cdot \hat{\boldsymbol{n}} \, \mathrm{d}S$ represents the radiation power in free space. The last two terms in (40) represent the energies stored in regions V_1 and V_2, respectively. Again, we can find that $\langle \boldsymbol{M}_n^*, \mathcal{R}^{\mathcal{M}} \boldsymbol{M}_n \rangle$ and $\langle \boldsymbol{M}_n^*, \mathcal{X}^{\mathcal{M}} \boldsymbol{M}_n \rangle$ represent the radiation power and stored energy, respectively, and evidently, $\mathcal{R}^{\mathcal{M}}$ is a semi-positive definite operator.

Similarly, a variational expression in terms of $\boldsymbol{M}_n$ gives the following generalised eigenvalue equation:

$$\mathcal{X}^{\mathcal{M}} \boldsymbol{M}_n = \lambda_n \mathcal{R}^{\mathcal{M}} \boldsymbol{M}_n \tag{43}$$

As both $\mathcal{R}^{\mathcal{M}}$ and $\mathcal{X}^{\mathcal{M}}$ are symmetric operators, all the eigenvalues λ_n and characteristic currents $\boldsymbol{M}_n$ are real. Therefore

$$\begin{aligned} \langle \boldsymbol{M}_n^*, (\mathcal{R}^{\mathcal{M}} + \mathrm{j}\mathcal{X}^{\mathcal{M}}) \boldsymbol{M}_n \rangle &= \langle \boldsymbol{M}_n, (\mathcal{R}^{\mathcal{M}} + \mathrm{j}\mathcal{X}^{\mathcal{M}}) \boldsymbol{M}_n \rangle \\ &= (1 + \mathrm{j}\lambda_n) \langle \boldsymbol{M}_n, \mathcal{R}^{\mathcal{M}} \boldsymbol{M}_n \rangle \end{aligned} \tag{44}$$

Evidently, the physical meanings of the eigenvalues are the same as those in Section 2. In addition, the physical meanings of the eigenvalues solved from (43) are also similar to that in the CM theory for PEC bodies [2].

Each characteristic current $\boldsymbol{M}_n$ can be normalised such that it radiates unit power

$$\langle \boldsymbol{M}_n, \mathcal{R}^{\mathcal{M}} \boldsymbol{M}_n \rangle = 1 \tag{45}$$

After normalisation, the orthogonality relationship among characteristic currents $\boldsymbol{M}_n$ is reduced to

$$\langle \boldsymbol{M}_m, \mathcal{Z}^{\mathcal{M}} \boldsymbol{M}_n \rangle = (1 + \mathrm{j}\lambda_n) \delta_{mn} \tag{46}$$

Similar to the derivations for (35), we can get the orthogonality relationship of the characteristic fields

$$\frac{1}{\eta_1} \int_{S_\infty} \boldsymbol{E}_m^{(1)} \cdot (\boldsymbol{E}_n^{(1)})^* \cdot \hat{\boldsymbol{n}} \, \mathrm{d}S = \delta_{mn} \tag{47}$$

Besides, it is worth noting that the eigenvalues and the characteristic currents solved under the two conditions $\boldsymbol{J}_n^S = 0$ and $\boldsymbol{M}_n^S = 0$ are the same. The difference is only in the computational procedure. Under the $\boldsymbol{J}_n^S = 0$ condition, characteristic electric currents are explicitly solved. Under the $\boldsymbol{M}_n^S = 0$ condition, characteristic magnetic currents are explicitly solved. Both of the two sets of modes satisfy orthogonality relationship over the infinite radiation sphere and the equivalent surfaces. The eigenvalues and modal significances solved under the two conditions give the same resonant frequencies of dielectric resonators.

4 Numerical results

Consider an isolated cylindrical dielectric resonator of radius 5.25 mm and height 4.6 mm. The relative dielectric constant is $\varepsilon_r = 38$. In general, modal significance is more convenient than eigenvalue to investigate the resonant behaviour over a wide frequency band. It is defined as [2, 4]

$$\mathrm{MS} = \left| \frac{1}{1 + \mathrm{j}\lambda_n} \right| \tag{48}$$

As can be seen, the modal significance transforms the $[-\infty, +\infty]$ value range of eigenvalues into a much smaller range of [0, 1]. Evidently, CMs with larger modal significance are in resonance and those with small modal significance are non-resonant modes.

Fig. 2 shows the modal significance solved from the proposed generalised eigenvalue equations. The curves with lines are solved from $\mathcal{X}^E \boldsymbol{J}_n = \lambda_n \mathcal{R}^E \boldsymbol{J}_n$, and the curves with scatters are solved from $\mathcal{X}^{\mathcal{M}} \boldsymbol{M}_n = \lambda_n \mathcal{R}^{\mathcal{M}} \boldsymbol{M}_n$. The resultant modal significances agree well with each other. The resultant modal fields and modal radiation patterns from the two generalised eigenvalue equations also achieve good agreement. The peaks of the modal significance clearly show the resonant frequencies of the dominant modes over the frequency band. It can be observed that this cylindrical resonator resonates in eight frequencies in the frequency band of 4.5–7.8 GHz. This conclusion is the same as that was reported in [30]. It illustrates that the proposed CM formulations are able to solve all the resonant modes over a given frequency band. However, the determinant root seeking method only found five resonant modes in the same frequency band [23]. Table 1 compares the resonant frequencies with those obtained from the determinant root seeking method and the measurement [22, 23]. It is observed that the resonant frequencies are very close to each

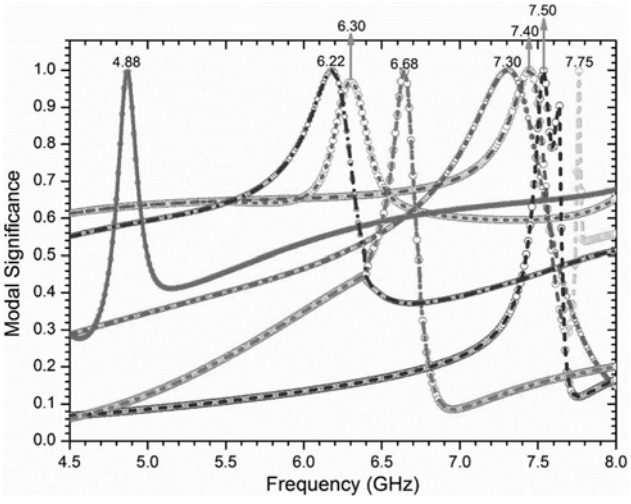

Fig. 2 *Modal significance of the isolated cylindrical dielectric resonator. Lines: computed from* $\mathcal{X}^E \boldsymbol{J}_n = \lambda_n \mathcal{R}^E \boldsymbol{J}_n$*; Scatters: computed from* $\mathcal{X}^{\mathcal{M}} \boldsymbol{M}_n = \lambda_n \mathcal{R}^{\mathcal{M}} \boldsymbol{M}_n$

Table 1 Comparison of the cylindrical DRA resonant frequencies obtained with the CM theory, measurement, and determinant root seeking method

Resonant modes	CM	Measured results [22]	Determinant root seeking method [23]
$TE_{01\delta}$	4.88	4.85	4.83
$HEM_{11\delta}$	6.30	—	6.33
$HEM_{12\delta}$	6.68	6.64	6.63
$TM_{01\delta}$	7.50	7.60	7.52
$HEM_{21\delta}$	7.75	7.81	7.75

Unit: GHz.

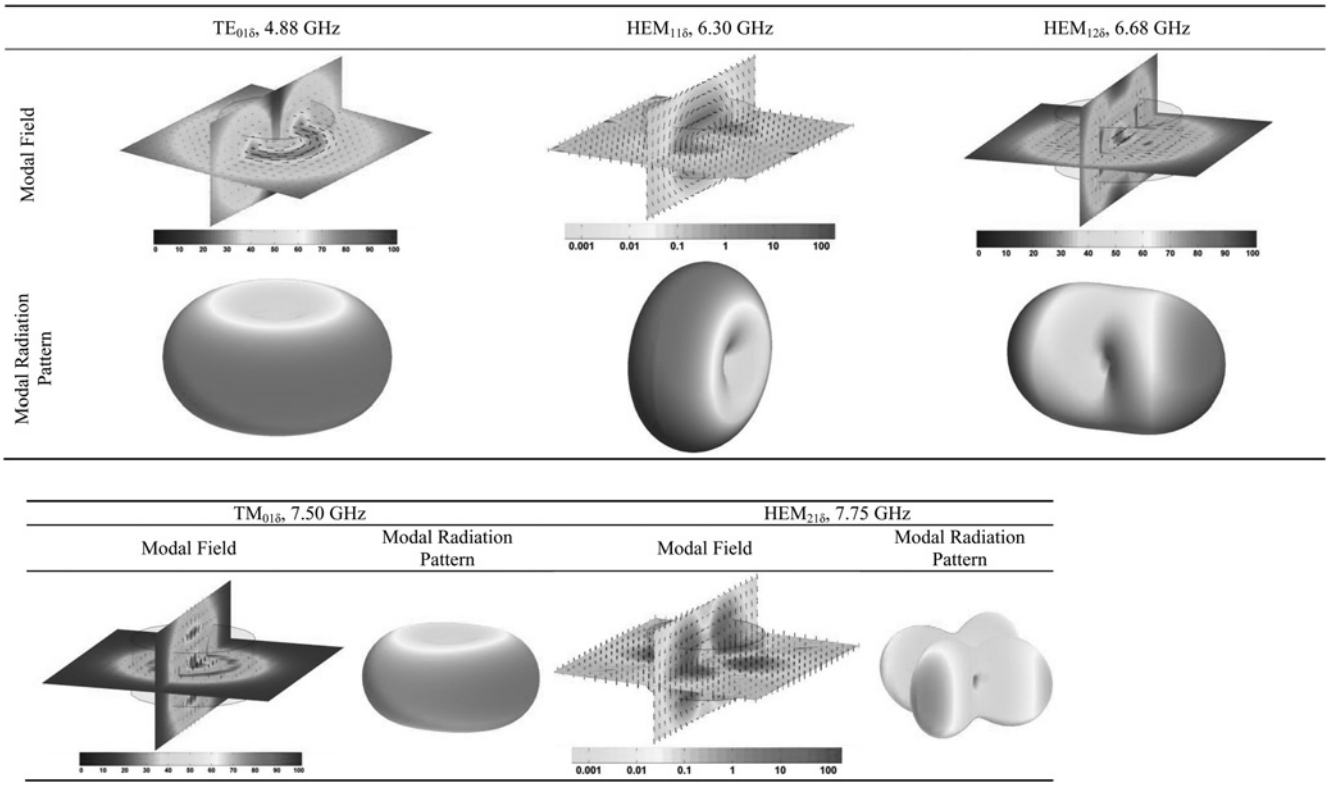

Fig. 3 *Modal fields and modal radiation patterns of the cylindrical DRA*

other. The errors of the CM results to the measured results are <1.3%.

Moreover, a classification of these resonant modes requires the calculations of the modal fields. Fig. 3 gives the modal fields and modal radiation patterns of the $TE_{01\delta}$ mode, $HEM_{11\delta}$ mode, $HEM_{12\delta}$ mode, $TM_{01\delta}$ mode, and $HEM_{21\delta}$ mode. As compared with the modal fields in [23], good agreement is observed. These modal fields provide valuable information on how to selectively excite each mode for specific radiation purpose.

As the second example, an isolated rectangular dielectric resonator as shown in Fig. 4 is considered. The dielectric constant is $\varepsilon_r = 10.0$. Fig. 5 shows the modal significance in the 3.1–5.6 GHz band. Again, from the peaks of the modal significance, one can observe the first three resonances at 3.41, 4.82, and 5.13 GHz, respectively. As can be observed from the modal fields in Fig. 6, the first three resonances are actually the TE^{y}_{111}mode, TE^{y}_{112} mode, and TE^{y}_{113} mode of the rectangular dielectric resonator. Besides, Fig. 5 also shows the modal significances for three higher-order modes. It can easily infer that these higher-order modes will resonant at much higher frequencies and will have their peaks at much higher frequencies. Table 2 compares the CM resonant frequencies with the measurement results and HFSS simulation results reported in [31]. It shows that the CM results agree well with the measured and simulated results given in [31]. The errors to the measurement results are <1.0%.

Fig. 6 presents the modal fields and modal radiation patterns of the isolated rectangular dielectric resonator antenna (DRA). As can be

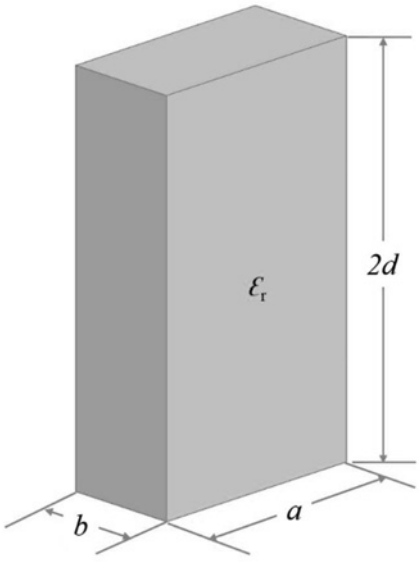

Fig. 4 *Configurations of the isolated rectangular dielectric resonator. a = 20.8 mm, b = 10.5 mm, d = 18.5 mm, $\varepsilon_r = 10.0$*

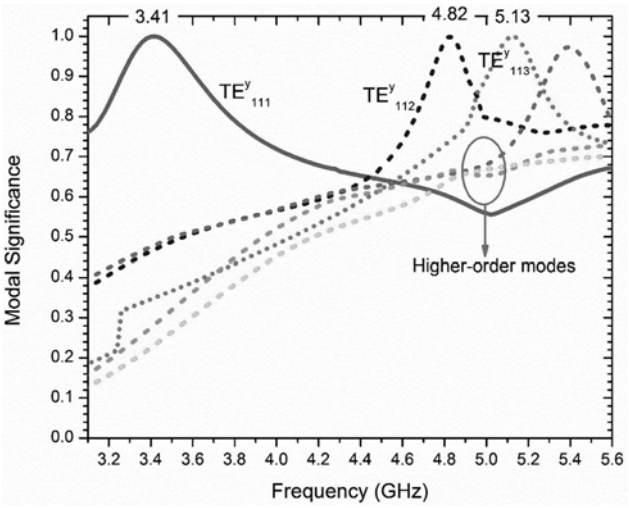

Fig. 5 *Modal significance of the isolated rectangular dielectric resonator*

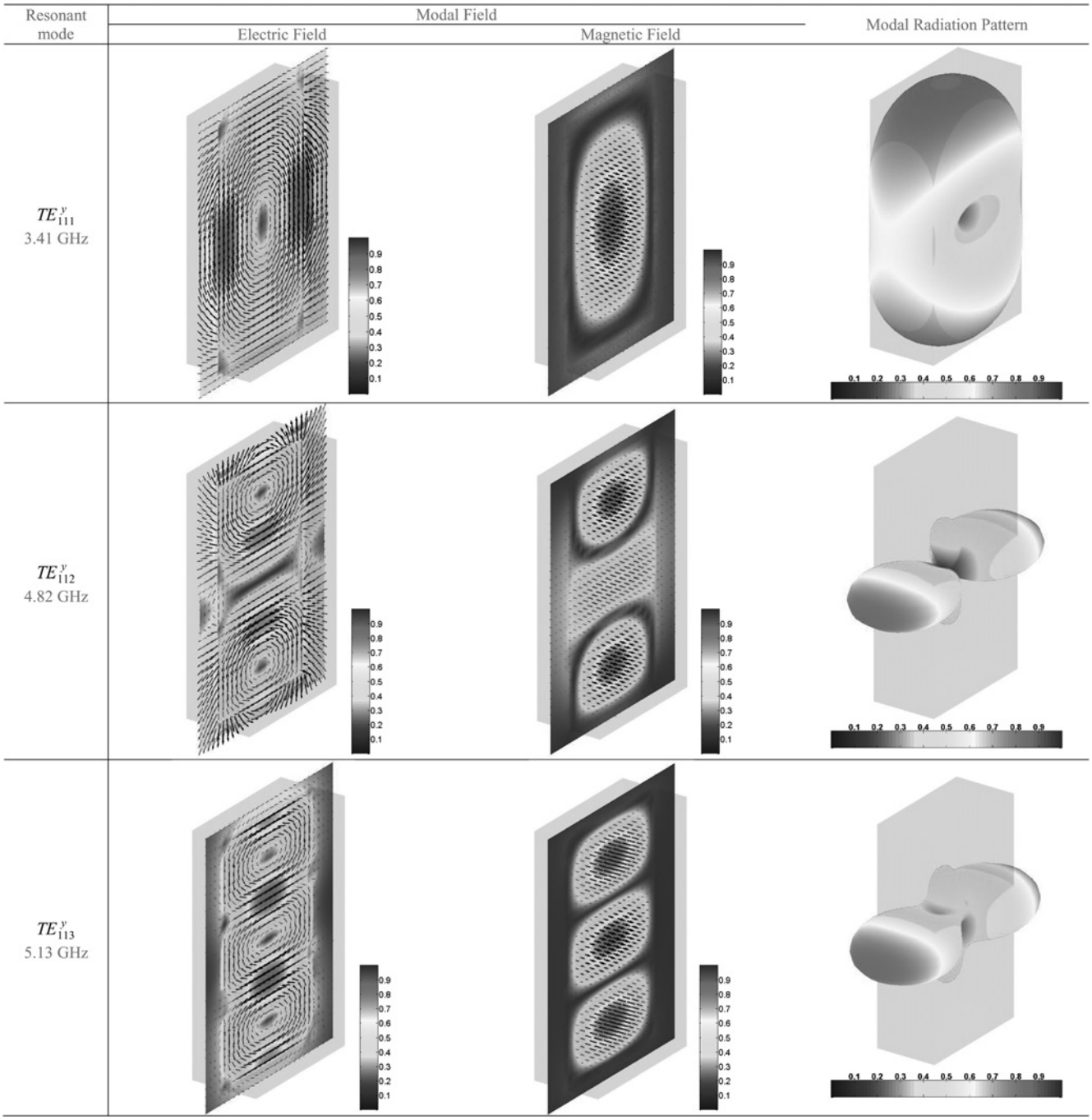

Fig. 6 *Modal fields and modal radiation patterns of the rectangular DRA*

observed, the modal fields of the three CMs agree well with the modal fields in Fig. 3 of [31]. The modal fields provide valuable guidelines on how to excite the radiating modes effectively. As the maximum magnetic field intensity of the TE^{y}_{111} mode and TE^{y}_{113} is at the surface with ground plane, a slot-coupling element (equivalent to a magnetic current) was introduced on the ground plane to provide efficient excitations for the two modes. However, the maximum magnetic field of the TE^{y}_{112} mode does not appear at the surface with ground plane. It cannot be excited through a slot-coupling element. Therefore, the dual-band rectangular DRA was realised by exciting the fundamental TE^{y}_{111} mode and the higher-order TE^{y}_{113} mode. This example shows that the modal fields clearly explain why the TE^{y}_{113} mode is used instead of the TE^{y}_{112} mode for dual-band DRA designs.

Table 2 Comparison of the rectangular DRA resonant frequencies obtained with the CM theory, measurement, and HFSS simulation with feeding structure

Resonant modes	Measured results, GHz [31]	CM		HFSS simulation [31]	
		Frequency, GHz	Error, %	Frequency, GHz	Error, %
TE^{y}_{111}	3.40	3.41	0.29	3.47	2.05
TE^{y}_{112}	—	4.82	—	—	—
TE^{y}_{113}	5.18	5.13	0.96	5.24	1.15

The two examples were simulated on a personal computer with a 3.4 GHz Intel Core and 8 GB RAM. Table 3 gives the central processing unit (CPU) time of the CM analysis at a single frequency. It shows that the CPU time for the two DRAs is <30 s. It is noted that the CPU time includes the time for the computation of the reduced matrix, solving the generalised eigenvalue equation, and the modal tracking procedure as discussed in [32]. Apparently, the CPU time is acceptable for such electrically small and medium

Table 3 CPU time for the CM analysis of the DRAs

	Cylindrical DRA	Rectangular DRA
number of triangle elements	206	698
number of unknowns	618	2094
number of modes	15	20
CPU time, s	2.59	25.15

The CPU time includes the time for the computation of the reduced matrix, solving the generalised eigenvalue equation, and the modal tracking procedure [32].

problems (MoM unknowns $\simeq 2000$). Therefore, the computational efficiency for such problems is good enough for DRA design using a common personal computer.

As discussed in the previous literature [2, 7], the developments of the CM theory (either for the conventional PEC problem [2, 7], or the dielectric problem discussed here) are intended for the analysis of electromagnetic problems with electrically small and medium sizes. In these problems, only a few modes are needed to characterise the radiation and scattering properties. However, for electrically large problems, there are too many closely spaced resonances to identify using the CM theory. Therefore, the CM theory is not so popular in the electrically large problems. In principle, however, CM analysis for the electrically large problems could be implemented using high-performance computing techniques through solving the generalised eigenvalue equations proposed in this paper.

5 Discussions and conclusions

This paper discusses the theory of CMs for dielectric resonators using the PMCHWT formulation. Following the Poynting's theorem, two generalised eigenvalue equations are developed for the CM analysis of dielectric resonators. The resultant CMs and eigenvalues have the same physical meanings as those in the CM theory for PEC bodies. Numerical results show that the developed CM theory is able to solve the resonant frequencies accurately for dielectric resonators. It is also capable of computing the internal modal fields and modal radiation patterns, which are of great importance in the excitation of a mode for specific radiation purpose.

In addition to the two new operators ($\mathcal{Z}^E$ and $\mathcal{Z}^{\mathcal{M}}$) and the corresponding generalised eigenvalue equations derived from the PMCHWT equation, one may also derive another two new operators by conducting similar manipulations to (11) and (12). However, they cannot provide physically meaningful CMs as in the $\mathcal{Z}^E$ and $\mathcal{Z}^{\mathcal{M}}$ cases. In the Appendix, we give mathematical proofs and physical explanations to show why they cannot work properly.

6 Acknowledgments

The author thanks Dr Chao-Fu Wang and Dr Fu-Gang Hu, Temasek Laboratories, National University of Singapore, for their discussions on the physical meanings of the eigenvalues in the newly proposed CM formulations.

7 References

1 Garbacz, R.J.: 'Modal expansions for resonance scattering phenomena', *Proc. IEEE*, 1965, **53**, (8), pp. 856–864
2 Harrington, R., Mautz, J.: 'Theory of characteristic modes for conducting bodies', *IEEE Trans. Antennas Propag.*, 1971, **19**, (5), pp. 622–628
3 Newman, E.H.: 'Small antenna location synthesis using characteristic modes', *IEEE Trans. Antennas Propag.*, 1979, **AP-21**, (4), pp. 530–531
4 Cabedo-Fabres, M., Antonio-Daviu, E., Valero-Nogueira, A., *et al.*: 'The theory of characteristic modes revisited: a contribution to the design of antennas for modern applications', *IEEE Antennas Propag. Mag.*, 2007, **49**, (5), pp. 52–68
5 Chen, Y., Wang, C.-F.: 'Characteristic mode analysis of PEC bodies using combined field integral equation'. 2015 IEEE AP-S Symp. on Antennas and Propagation and URSI CNC/USNC Joint Meeting (AP-S/URSI 2015), Vancouver, BC, Canada, July 2015, pp. 1474–1475
6 Chen, Y., Wang, C.-F.: 'Electrically small UAV antenna design using characteristic modes', *IEEE Trans. Antennas Propag.*, 2014, **62**, (2), pp. 535–545
7 Chen, Y., Wang, C.-F.: 'HF band shipboard antenna design using characteristic modes', *IEEE Trans. Antennas Propag.*, 2015, **63**, (3), pp. 1004–1013
8 Chen, Y., Wang, C.-F.: 'Shipboard NVIS radiation system design using the theory of characteristic modes'. IEEE Int. Symp. on Antennas and Propagation, Memphis, USA, 6–11 July 2014, pp. 852–853
9 Chen, Y., Wang, C.-F.: 'Characteristic mode synthesis of omni-directional radiation patterns for electrically small UAV'. 2015 IEEE AP-S Symp. on Antennas and Propagation and URSI CNC/USNC Joint Meeting (AP-S/URSI 2015), Vancouver, BC, Canada, July 2015, pp. 1430–1431
10 Chen, Y., Wang, C.-F.: 'Synthesis of platform integrated antennas for reconfigurable radiation patterns using the theory of characteristic modes'. The 10th Int. Symp. on Antennas and Propagation EM Theory (ISAPE), Xi'an, China, October 2012, pp. 281–285
11 Li, H., Tan, Y., Lau, B.K., *et al.*: 'Characteristic mode based tradeoff analysis of antenna-chassis interactions for multiple antenna terminals', *IEEE Trans. Antennas Propag.*, 2012, **60**, (2), pp. 490–502
12 Li, H., Miers, Z., Lau, B.K.: 'Design of orthogonal MIMO handset antennas based on characteristic mode manipulation at frequency bands below 1 GHz', *IEEE Trans. Antennas Propag.*, 2014, **62**, (5), pp. 2756–2766
13 Miers, Z., Li, H., Lau, B.K.: 'Design of bandwidth enhanced and multiband MIMO antennas using characteristic modes', *IEEE Antennas Wirel. Propag. Lett.*, 2013, **12**, pp. 1696–1699
14 Chen, Y., Wang, C.-F.: 'Characteristic-mode-based improvement of circularly polarized U-slot and E-shaped patch antennas', *IEEE Antennas Wirel. Propag. Lett.*, 2012, **11**, pp. 1474–1477
15 Chen, Y., Wang, C.-F.: 'Synthesis of reactively controlled antenna arrays using characteristic modes and DE algorithm', *IEEE Antennas Wirel. Propag. Lett.*, 2012, **11**, pp. 385–388
16 Chen, Y., Wang, C.-F.: 'Electrically loaded Yagi-Uda antenna optimizations using characteristic modes and differential evolution', *J. Electromagn. Waves Appl.*, 2012, **26**, (8–9), pp. 1018–1028
17 Wu, W., Zhang, Y.P.: 'Analysis of ultra-wideband printed planar quasi-monopole antennas using the theory of characteristic modes', *IEEE Antennas Propag. Mag.*, 2010, **52**, (6), pp. 67–77
18 Antonino-Daviu, E., Fabres, M., Ferrando-Bataller, M., *et al.*: 'Modal analysis and design of band-notched UWB planar monopole antennas', *IEEE Trans. Antennas Propag.*, 2010, **58**, (5), pp. 1457–1467
19 Cabedo-Fabres, M., Antonino-Daviu, E., Valero-Nogueira, A., *et al.*: 'Analysis of wide band planar monopole antennas using characteristic modes'. IEEE Int. Symp. on Antennas Propag., Columbus, USA, June 2003, pp. 733–736
20 Harrington, R., Mautz, J., Chang, Y.: 'Characteristic modes for dielectric and magnetic bodies', *IEEE Trans. Antennas Propag.*, 1972, **20**, (2), pp. 194–198
21 Chang, Y., Harrington, R.: 'A surface formulation for characteristic modes of material bodies', *IEEE Trans. Antennas Propag.*, 1977, **25**, (6), pp. 789–795
22 Glisson, A.W., Kajfez, D., James, J.: 'Evaluation of modes in dielectric resonators using a surface integral equation formulation', *IEEE Trans. Microw. Theory Tech.*, 1983, **31**, (12), pp. 1023–1029
23 Kajfez, D., Glisson, A.W., James, J.: 'Computed modal field distributions for isolated dielectric resonators', *IEEE Trans. Microw. Theory Tech.*, 1984, **32**, (12), pp. 1609–1616
24 Liu, Y., Safavi-Naeini, S., Chaudhuri, S.K., *et al.*: 'On the determination of resonant modes of dielectric objects using surface Integral equations', *IEEE Trans. Antennas Propag.*, 2004, **52**, (4), pp. 1062–1069
25 Chen, Y., Wang, C.-F.: 'Surface integral equation based characteristic mode formulation for dielectric resonators'. 2014 IEEE Antennas and Propagation Society Int. Symp. (APSURSI), Memphis, USA, July 2014, pp. 846–847
26 Poggio, A.J., Miller, E.K.: 'Integral equation solutions of three dimensional scattering problems', in Mittra, R., (Eds.): 'Computer techniques for electromagnetics' (Permagon, 1973)
27 Wu, T.-K., Tsai, L.L.: 'Scattering from arbitrarily-shaped lossy dielectric bodies of revolution', *Radio Sci.*, 1977, **12**, (5), pp. 709–718
28 Love, A.E.H.: 'The integration of equations of propagation of electric waves', *Philos. Trans. R. Soc. London, Ser. A*, 1901, **197**, pp. 1–45
29 Harrington, R.F.: 'Fundamental concepts', in Harrington, R.F. (Ed.): 'Time-harmonic electromagnetic fields' (Wiley-IEEE Press, 2001), pp. 19–23
30 Mongia, R.K.: 'Theoretical and experimental resonant frequencies of rectangular dielectric resonators', *IEE Proc. H, Microw. Antennas Propag.*, 1992, **139**, (1), pp. 98–104
31 Fang, X.S., Leung, K.W.: 'Designs of single-, dual-, wide-band rectangular dielectric resonator antennas', *IEEE Trans. Antennas Propag.*, 2011, **59**, (6), pp. 2409–2414
32 Raines, B.D., Rojas, R.G.: 'Wideband characteristic mode tracking', *IEEE Trans. Antennas Propag.*, 2012, **60**, (7), pp. 3537–3541

8 Appendix

Mathematically, there are another two operators that can be derived from (11) and (12). From (12) and the assumption of $\boldsymbol{J}_n^S = 0$ on surface S, the $\boldsymbol{J}_n$ can be expressed in terms of the $\boldsymbol{M}_n$

$$\boldsymbol{J}_n = -(\mathcal{Z}^{\mathcal{HJ}})^{-1}\mathcal{Z}^{\mathcal{HM}}\boldsymbol{M}_n \tag{49}$$

Substituting $\boldsymbol{J}_n = -(\mathcal{Z}^{\mathcal{HJ}})^{-1}\mathcal{Z}^{\mathcal{HM}}\boldsymbol{M}_n$ into (11), we have

$$\left(\mathcal{Z}^{\mathcal{EM}} - \mathcal{Z}^{\mathcal{EJ}}(\mathcal{Z}^{\mathcal{HJ}})^{-1}\mathcal{Z}^{\mathcal{HM}}\right)\boldsymbol{M}_n = \mathcal{Z}^{\mathcal{A}1}\boldsymbol{M}_n \tag{50}$$

where

$$\mathcal{Z}^{\mathcal{A}1} = \mathcal{Z}^{\mathcal{EM}} - \mathcal{Z}^{\mathcal{EJ}}(\mathcal{Z}^{\mathcal{HJ}})^{-1}\mathcal{Z}^{\mathcal{HM}} \tag{51}$$

Apparently, $\mathcal{Z}^{\mathcal{A}1} \neq (\mathcal{Z}^{\mathcal{A}1})^{\mathrm{T}}$, that is, $\mathcal{Z}^{\mathcal{A}1}$ is not a symmetric operator.

In addition, if we try to find the characteristic equivalent surface magnetic current $\boldsymbol{M}_n$ using $\mathcal{Z}^{\mathcal{A}1}$, the inner product $\langle \boldsymbol{M}_n^*, \mathcal{Z}^{\mathcal{A}1}\boldsymbol{M}_n\rangle$ must have clear physical explanations to the complex power of the system. Similar to the derivations in (27) and (42), $\langle \boldsymbol{M}_n^*, \mathcal{Z}^{\mathcal{A}1}\boldsymbol{M}_n\rangle$ can be written as

$$\begin{aligned}\langle \boldsymbol{M}_n^*, \mathcal{Z}^{\mathcal{A}1}\boldsymbol{M}_n\rangle &= \langle \boldsymbol{M}_n^*, \mathcal{Z}^{\mathcal{EJ}}\boldsymbol{J}_n + \mathcal{Z}^{\mathcal{EM}}\boldsymbol{M}_n\rangle \\ &= -\langle \boldsymbol{M}_n^*, \boldsymbol{E}_n^{(1)} - \boldsymbol{E}_n^{(2)}\rangle \\ &= -\langle -\hat{\boldsymbol{n}} \times (\boldsymbol{E}_n^{(1)})^*, \boldsymbol{E}_n^{(1)}\rangle + \langle \hat{\boldsymbol{n}} \times (\boldsymbol{E}_n^{(2)})^*, \boldsymbol{E}_n^{(2)}\rangle \\ &= \int_S (\boldsymbol{E}_n^{(1)})^* \times \boldsymbol{E}_n^{(1)} \cdot \hat{\boldsymbol{n}}\,\mathrm{dS} - \int_S (\boldsymbol{E}_n^{(2)})^* \times \boldsymbol{E}_n^{(2)} \cdot \hat{\boldsymbol{n}}\,\mathrm{dS}\end{aligned} \tag{52}$$

Evidently, $\langle \boldsymbol{M}_n^*, \mathcal{Z}^{\mathcal{A}1}\boldsymbol{M}_n\rangle$ does not represent the complex power in the system. Therefore, the generalised eigenvalue equation derived from $\mathcal{Z}^{\mathcal{A}1}$ cannot provide CMs with clear physical meanings.

Similarly, we can derive another operator from (11) and (12) with consideration of the assumption of $\boldsymbol{M}_n^S = 0$ on surface S. From (11), the $\boldsymbol{M}_n$ can be written as

$$\boldsymbol{M}_n = -(\mathcal{Z}^{\mathcal{EM}})^{-1}\mathcal{Z}^{\mathcal{EJ}}\boldsymbol{J}_n \tag{53}$$

Substituting $\boldsymbol{M}_n = -(\mathcal{Z}^{\mathcal{EM}})^{-1}\mathcal{Z}^{\mathcal{EJ}}\boldsymbol{J}_n$ into (12), we have

$$\left(\mathcal{Z}^{\mathcal{HJ}} - \mathcal{Z}^{\mathcal{HM}}(\mathcal{Z}^{\mathcal{EM}})^{-1}\mathcal{Z}^{\mathcal{EJ}}\right)\boldsymbol{J}_n = \mathcal{Z}^{\mathcal{A}2}\boldsymbol{J}_n \tag{54}$$

where

$$\mathcal{Z}^{\mathcal{A}2} = \mathcal{Z}^{\mathcal{HJ}} - \mathcal{Z}^{\mathcal{HM}}(\mathcal{Z}^{\mathcal{EM}})^{-1}\mathcal{Z}^{\mathcal{EJ}} \tag{55}$$

We can also observe that $\mathcal{Z}^{\mathcal{A}2}$ is not a symmetric operator.

Again, if we try to solve the characteristic equivalent surface electric current using $\mathcal{Z}^{\mathcal{A}2}$, the inner product $\langle \boldsymbol{J}_n^*, \mathcal{Z}^{\mathcal{A}2}\boldsymbol{J}_n\rangle$ must have clear physical explanations to the complex power of the system. Similar to the derivations in (24) and (39), $\langle \boldsymbol{J}_n^*, \mathcal{Z}^{\mathcal{A}2}\boldsymbol{J}_n\rangle$ can be written as

$$\begin{aligned}\langle \boldsymbol{J}_n^*, \mathcal{Z}^{\mathcal{A}2}\boldsymbol{J}_n\rangle &= \langle \boldsymbol{J}_n^*, \mathcal{Z}^{\mathcal{HJ}}\boldsymbol{J}_n + \mathcal{Z}^{\mathcal{HM}}\boldsymbol{M}_n\rangle \\ &= -\langle \boldsymbol{J}_n^*, \boldsymbol{H}_n^{(1)} - \boldsymbol{H}_n^{(2)}\rangle \\ &= -\langle \hat{\boldsymbol{n}} \times (\boldsymbol{H}_n^{(1)})^*, \boldsymbol{H}_n^{(1)}\rangle + \langle \hat{\boldsymbol{n}} \times (\boldsymbol{H}_n^{(2)})^*, \boldsymbol{H}_n^{(2)}\rangle \\ &= \int_S \boldsymbol{H}_n^{(1)} \times (\boldsymbol{H}_n^{(1)})^* \cdot \hat{\boldsymbol{n}}\,\mathrm{dS} - \int_S \boldsymbol{H}_n^{(2)} \times (\boldsymbol{H}_n^{(2)})^* \cdot \hat{\boldsymbol{n}}\,\mathrm{dS}\end{aligned} \tag{56}$$

It is also evident to see that $\langle \boldsymbol{J}_n^*, \mathcal{Z}^{\mathcal{A}2}\boldsymbol{J}_n\rangle$ does not represent the complex power in the system. Therefore, the generalised eigenvalue equation derived from $\mathcal{Z}^{\mathcal{A}2}$ cannot provide CMs with clear physical meanings.